The First H I-Discovered Galaxy in the Bootes Void

Szomoru, A; van Gorkom, JH; Gregg, M; de Jong, RS

Published in:
The Astronomical Journal

Publication date:
1993

THE FIRST H I-DISCOVERED GALAXY IN THE BOOTES VOID

A. SZOMORU
Kapteyn Astronomical Institute, P.O. Box 800, NL 9700 AV Groningen, The Netherlands

J. H. VAN GORKOM
Department of Astronomy, Columbia University, New York, New York 10027

M. GREGG
Mt. Stromlo Observatory, Private Bag, Weston Creek, A.C.T. 2611, Australia

R. S. DE JONG
Kapteyn Astronomical Institute, P.O. Box 800, NL 9700 AV Groningen, The Netherlands

Received 27 May 1992; revised 21 September 1992

ABSTRACT

In this paper we present a detailed study of the first H I-discovered galaxy in the Boötes void, at a distance of 145.5 Mpc. We have observed this galaxy both at low and high resolution in the 21 cm line and optically. The galaxy has an irregular, slowly rotating H I disk. The gas is much more extended than the optical disk, extending out as far as 6.4 times R_{25}. The rotation curve of the galaxy is flat: amplitude and shape can be explained by the presence of a dark halo with a mass of 1.6 times the luminous mass.

1. INTRODUCTION

The possible existence of a large void in the distribution of optically bright galaxies in the direction of Boötes was first discussed in 1981 by Kirshner and collaborators (Kirshner *et al.* 1981). Redshift measurements of galaxies in three small fields 35° apart showed an identical gap in the velocity distribution around 15 000 km s^{-1}. A subsequent redshift survey confirmed the existence of this void (Kirshner *et al.* 1987). In this survey, redshifts of 239 galaxies in 283 fields distributed between the original three fields were measured. Assuming a uniform velocity distribution, 31 galaxies should have been detected within the redshift range of the void. As none were found, they concluded that the density of the void can be no higher than one-quarter of the cosmic mean.

The largest sphere devoid of galaxies consistent with their data has a radius of 31 Mpc and is centered at $\alpha = 14^{h}50^{m}$, $\delta = +46°$, at a mean redshift of 15 500 km s^{-1}, which implies a volume of 1.25×10^{5} Mpc^{3}.[1] This is what is commonly called the Boötes void.

This void has been the subject of a large number of investigations. In objective prism surveys a total of eight emission line galaxies were detected (Sanduleak & Pesch 1982, 1987; Moody 1986; Moody *et al.* 1987; Tifft *et al.* 1986; Weistrop & Downes 1988; Weistrop 1987). Additionally, two galaxies known from the literature, Mkn 845 and the compact galaxy IZw 81, were found to lie within the boundaries of the void. More recently, Bothun & Aldering (1988) and Dey *et al.* (1990) have discovered 26 more void galaxies, selecting their candidates from the *IRAS* survey. Dey *et al.* find the density of *IRAS* galaxies in the void to lie between 1/6 and 1/3 of the mean, consistent with the original estimate of the void density by Kirshner *et al.* (1987).

Nearly all galaxies found in this void were selected by their strong emission lines or *IRAS* flux. As a result they form a somewhat peculiar and certainly biased sample. Although all morphological types of galaxies are present in clusters as well as in the field, there is a clear trend of type with environment. This trend, in which ellipticals and SOs inhabit the densest regions while irregulars and late-type spirals populate the field is well established (Oemler 1974; Dressler 1980; Postman & Geller 1983). If this trend can be extrapolated to regions of extreme low density, the population of the void should consist mainly of gas-rich late-type systems. Consequently a survey in the 21 cm line, though biased in its own way, might throw some light on the "normal" population of the void.

The first 21 cm line observations of the Boötes void were done in 1989 December and 1990 January using the Very Large Array (VLA)[2] (Napier *et al.* 1983) in D configuration. These observations were pointed at known void galaxies. Most of them proved to have large H I masses and were easily detected, in spite of their distance. In addition we discovered a number of uncatalogued H I-rich companion galaxies. The results of these observations and of a subsequent survey will be published at a later date (Szomoru *et al.*, in preparation).

The first uncatalogued galaxy detected in H I is a companion to the void object CG 1517+39 (Moody *et al.*

[1]Throughout this paper, we have assumed $H_0 = 100$ km s^{-1} Mpc^{-1}.

[2]The NRAO is operated by Associated Universities, Inc., under a cooperative agreement with the National Science Foundation.

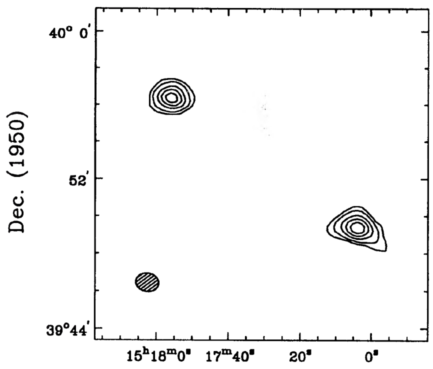

FIG. 1. Contour plot of the total H I emission of CG 1517+39 (upper left) and BHI 1517+39, corrected for primary beam attenuation. The contours are 0.2 (3σ), 0.4, 0.8, 1.2, and 1.6×10^{20} cm^{-2}. The resolution is $58.6''\times74.8''$. The size of the beam is indicated in the lower left corner.

1987). Figure 1 shows a total H I image of the two galaxies, obtained with the VLA in D array. Their angular separation is 12′, corresponding to a projected distance of about 0.5 Mpc, their redshifts differ by less than 100 km s^{-1}. Both systems are gas rich and clearly show rotation. The companion is just barely resolved at the resolution of the VLA in D configuration. As the synthesized beam in this configuration has a full width at half-maximum of 1′, this implies an H I diameter of at least 40 kpc. The optical counterpart, on the POSS plate, is fairly faint and resembles an irregular galaxy. The other H I-detected companions tend to be similar: they possess large H I masses, in some cases they show rotation, and their magnitudes are of the order of 16–17 (as estimated from the POSS plates).

To determine whether these void galaxies differ from field galaxies is important for theories of galaxy formation and evolution. The absence of interactions between galaxies in such an extremely underdense region might lead to retarded star formation and undisturbed, extended H I disks. It has also been suggested (Hoffman *et al.* 1992) that initial conditions can have a strong influence on the structure of galaxies, causing massive low-surface density galaxies like Malin I to form in voids.

We have reobserved CG 1517+39 and companion at higher resolution, to obtain detailed information on their kinematics and gas morphology. In addition we obtained broadband photometry. This paper will deal specifically with the uncatalogued companion, which we name BHI 1517+39.

2. OBSERVATIONS, DATA REDUCTION

2.1 21 Centimeter Line Observations

BHI 1517+39 was discovered in 1990 January during a 6 hr observing run with the VLA in D array. In 1990 August we reobserved this galaxy with the VLA in B array for 24 h, divided in three runs of 8 h each. The observational parameters are listed in Table 1.

TABLE 1. Parameters of VLA observations.

Configuration	D	B
Date	January 1990	August 1990
No. telescopes	27	27
No. hours	6	3 × 8
No. IF's	2	2
Total bandwidth	3.125 MHz	3.125 MHz
Field center (1950) RA	15h17m56s	15h17m30s
Dec	39°56′27.0″	39°53′00.0″
Central velocity (heliocentric)	14261.2 km s^{-1}	14185.6 km s^{-1}
No. channels	64	64
Shortest spacing	0.033 km	0.21 km
Longest spacing	1.03 km	11.4 km
Largest structure visible	15′	2′
FWHM synthesized beam	74.8″ × 58.6″	15″ × 15″
FWHM primary beam	30′	30′
Velocity resolution (after Hanning smoothing)	22.6 km s^{-1}	22.6 km s^{-1}
r.m.s. noise	0.5 mJy/beam	0.44 mJy/beam
Conversion mJy/beam–Kelvin: equivalent of 1 mJy/beam	0.15 K	2.95 K

2.1.1 D array

The UV data were calibrated and processed into a cube of images. As the line emission of the two galaxies extends all the way to one edge of the band, only channels at the other side of the band could be used for a continuum image; 21 channels at the low frequency side were averaged and subtracted from the cube. To achieve the best possible signal-to-noise ratio, natural weighting was applied in making images. The rms noise in the images, after Hanning smoothing to a resolution of 22.6 km s^{-1}, was 0.5 mJy/beam.

2.1.2 B array

The data of the three runs were calibrated separately. After calibration, the UV databases were combined and processed. The continuum emission was subtracted using the AIPS task UVLIN, which fits and subtracts the continuum in the UV plane. Twenty line-free channels at the high and low frequency side of the H I signal were used for this fit.

As in the case of the D-array data, natural weighting was applied in making images. The original resolution was $6.7''\times6.7''$; to improve the signal to noise ratio we smoothed the data both spatially and in velocity. Channel maps with emission were CLEANed and restored with a Gaussian beam. In the final images the rms noise, at a resolution of 22.6 km s^{-1} and $15''\times15''$, is 0.44 mJy/beam. The 5σ H I-detection limit per independent channel, at a distance of 155 Mpc, is $2.8\times10^{8}\,\mathcal{M}_{\odot}$. This means that a Magellanic-Cloud-type system would easily have been detected.

We show channel images smoothed to a resolution of $20''\times20''$; the rms noise in these images is 0.53 mJy/beam. Our typical column density sensitivity at this resolution is 2.7×10^{19} cm^{-2}.

A radio continuum image was made as well: the strongest continuum source in the field is a point source with a flux density of 36.5 mJy. After CLEANing, the rms noise in the image was 0.15 mJy/beam. At the position of BHI 1517+39 no continuum emission above 3σ is detectable.

2.2 Optical Observations

BVI broadband photometry was obtained in 1991 April with the 1 m Jacobus Kapteyn Telescope on La Palma, seeing varied between 1.4″ and 1.8″. We used a GEC CCD with 385×578 pixels and a pixel size of 0.3″. Integration times were 1200 s for *B*, 600 for *V* and *I*. Twilight skyflats were used for flatfielding. Sky subtraction was performed by fitting a second-order polynomial surface to the sky surrounding the galaxy. The standard fields of M67 (Schild 1983), M92, and N4147 (Cristian *et al.* 1985) were used for calibration. The estimated zero point errors for this night were 0.09 *B* mag, 0.05 *V* mag, and 0.06 *I* mag. Total magnitudes were calculated by integrating over a 30″ diameter circular area. Magnitudes were corrected for galactic absorption following the precepts of Burstein and Heiles (1984); this correction is only 0.03 mag in the *B* band.

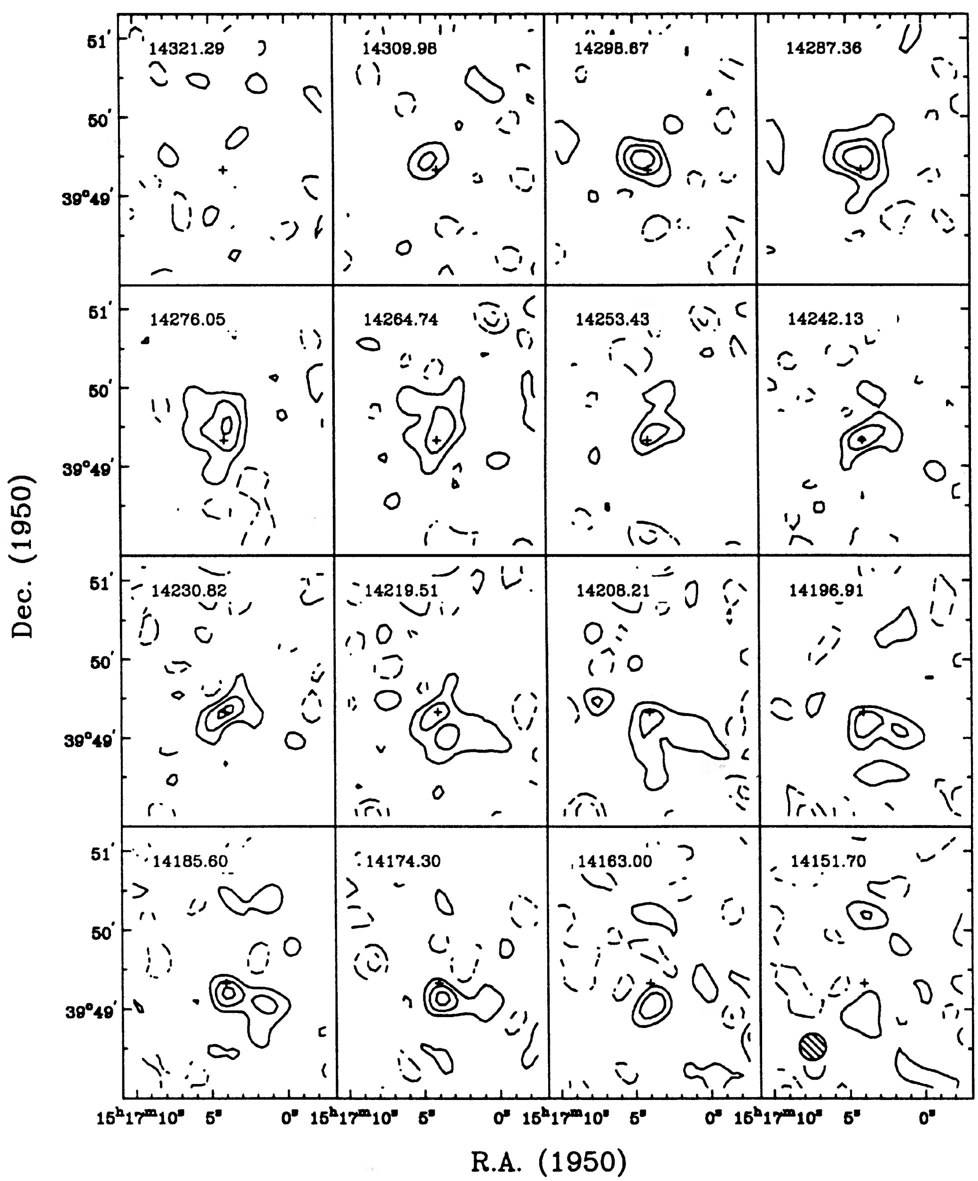

FIG. 2. Mosaic of channel maps of the continuum subtracted cleaned 21 cm line emission for BHI 1517+39. The contour levels are −1.54, −0.77, 0.77 (1.5σ), 1.54, 2.31, and 3.08 mJy/beam. The heliocentric velocities (in km s^{-1}) are listed in the upper left corner of each map. The size of the beam (20″×20″) is indicated in the lower left corner of the last image. The crosses indicate the center of the galaxy.

2.3 *Relativistic Corrections*

At the redshift of the Boötes void, relativistic effects become important. As most H I observations are done at very low redshift, these corrections are hardly ever applied to H I data; to avoid confusion we list the corrections explicitly.

In our H I observations, we used the optical velocity definition,

$$V_{\rm opt}=\frac{\lambda-\lambda_0}{\lambda_0}\,c=\frac{\nu_0-\nu}{\nu}\,c=zc,$$

with c the speed of light and ν_0 the rest frequency of the observed line.

As distance we took the luminosity distance, which is the proper distance $d_{\rm prop}=c\{q_0z+[q_0-1][(1+2q_0z)^{0.5}-1]\}/q_0^2H_0(1+z)$ (Sandage 1975) multiplied by $(1+z)$ to correct for loss of energy of the photons due to their redshift and time dilation, $d_{\rm lum}=d_{\rm prop}(1+z)$, corrected for solar motion with respect to the velocity centroid of the Local Group: $D=d_{\rm lum}+300\sin(l)\cos(b)/H_0$. This distance was used for calculating the H I mass using the standard formula

$$M_{\rm H\,I}/\mathscr{M}_\odot=2.36\times10^5D^2\int S dv,$$

with D in Mpc, v the width of the line in km s^{-1}, and S the flux density in Jy.

The measured optical flux has to be multiplied by one more factor $(1+z)$ to correct for the difference in bandwidth in observed and rest frames. The 21 cm flux does not need such a correction, as the whole line is observed. A complete K correction would additionally require a correction for the luminosity change as a function of wavelength, but we have chosen not to apply this correction. All quantities were calculated with $q_0=0.5$.

3. H I PROPERTIES

3.1 *Channel Images, Global Profile*

The CLEANed channel images are shown in Fig. 2, at a resolution of 20″×20″.

The global H I profile (Fig. 3) clearly shows a double peak, typical for a disk in differential rotation. The profile is slightly asymmetrical. The systemic heliocentric velocity obtained from the midpoint velocities at 50% and 20% is 14 234 km s^{-1}.

3.2 *Total H I Image*

Figure 4 shows a contour plot of the total H I emission, superposed on a gray scale B-band image. This image was constructed by applying a 1.5σ cutoff to the 20″×20″ resolution images. Areas with signal above this cutoff were then used as a mask for the higher resolution images. The H I disk is much more extended than the optical disk, the peak of the H I emission coincides with the center of the optical galaxy. On the southwest side of the galaxy the gas is extended out to a radius of 50″, corresponding to 35 kpc. The H I diameter, measured along the major axis, is 49″±2″ at a density of 1.34×10^{20} cm^{-2}. The position angle of the major axis was determined from the optical data, as will be described later.

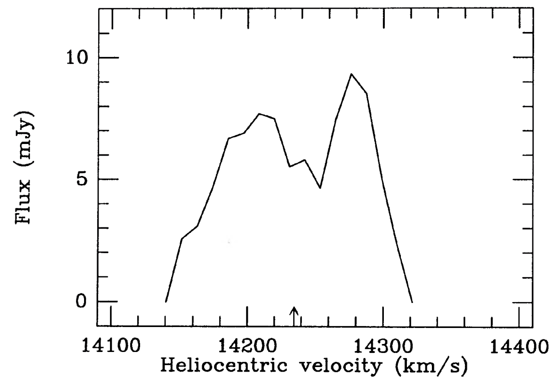

FIG. 3. Global H I profile of BHI 1517+39. The flux densities are corrected for primary beam attenuation. The adopted heliocentric systemic velocity is indicated with an arrow.

We also constructed a total H I image from the D-array data, by blanking areas without emission in the Hanning smoothed cube. In Fig. 5, we plot a superposition of the two total H I images; the low resolution data confirm the existence of the large H I extension seen at higher resolution. The D array shows a low surface brightness envelope of H I; taking into account the large beam size we estimate the maximum extent to be 85 kpc, at a level of approximately 5×10^{19} cm^{-2}. The total flux density derived from the D-array data is 6% larger than the B-array flux density; the two flux densities agree within the errors.

3.3 *Velocity Field, Rotation Curve*

In Fig. 6 the velocity field is shown. This velocity field was constructed by interactively fitting Gaussians to the

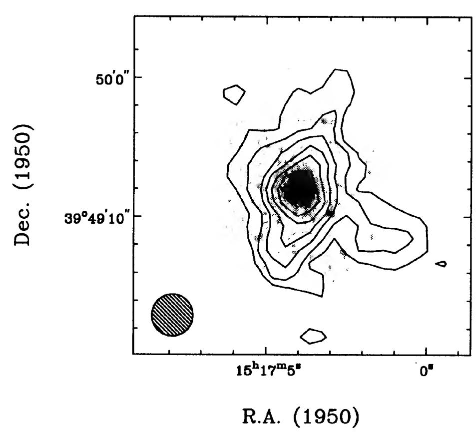

FIG. 4. Contour plot of the total H I emission of BHI 1517+39, corrected for primary beam attenuation, superposed on a gray-scale B-band image. The contours are 1.34 (1.5σ), 2.67, 4.53, 6.39, 8.24, 10.10, and 11.95 $\times10^{20}$ cm^{-2}, the lowest visible level in the gray scale is approximately 25 mag arcsec^{-2}. The cross indicates the center of the galaxy, the resolution is 15″×15″, indicated in the left bottom corner.

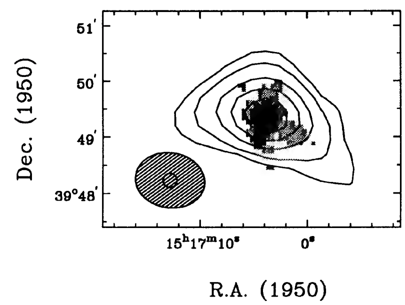

FIG. 5. Superposition of the total H I images obtained from D- and B-array data. The contours are 0.2 (3σ), 0.4, 0.8, 1.2, and 1.6×10^{20} cm^{-2}, the outer gray scale corresponds to 1.34 $\times10^{20}$ cm^{-2}. The large ellipse indicates the resolution of the D array, 58.6″×74.8″, the B-array beam (15″×15″) is plotted inside this ellipse.

velocity profiles at each pixel position of the B-array cube. The isovelocity contours are clearly twisted; this could be caused by a warped disk. The low resolution D-array data seem to confirm this.

Figure 7 shows a position-velocity map along the major axis of the galaxy. Plotted in the position-velocity map is the rotation curve as estimated by eye, following the ridge of H I emission. The uncertainty in the projected rotational velocity is ±5 km s^{-1}. To better determine the shape of the rotation curve, we used high resolution dirty (not CLEANed) images in making this image. The resolution in this case is 10″×10″.

At a radius of about 10″ the rotation curve on the north side flattens, and may even be declining farther out. On the south side of the galaxy the rotation curve continues to increase smoothly out to at least 20″, but clearly flattens on this side too.

By averaging the velocities of approaching and receding

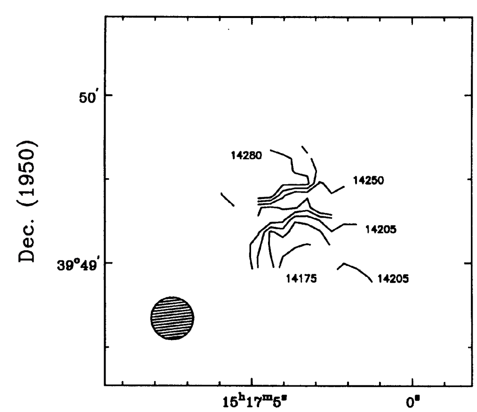

FIG. 6. Velocity field of BHI 1517+39, obtained by fitting Gaussians to the velocity profiles at each pixel position. The resolution is 15″×15″, indicated in the left bottom corner.

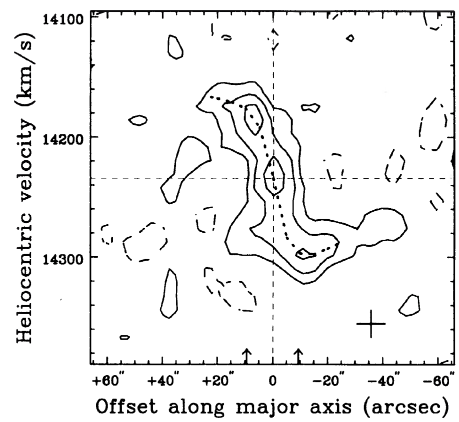

FIG. 7. Position-velocity map along the major axis of BHI 1517+39, at a position angle of 36.6°. The contour levels are −1, −0.50, 0.50 (1.5σ), 1, and 1.5 mJy/beam. The dots trace the rotation curve, as estimated by eye, the arrows indicate the position of R_{25}. The resolution is indicated by the cross in the lower right corner.

sides and correcting the resulting velocities for inclination, we construct a mean rotation curve (Fig. 8). The error bars of the first two points denote the deprojected uncertainty (±7.5 km s^{-1}), the error bar of the last point denotes the difference between approaching and receding velocities, as this difference is larger than the uncertainty (±11.4 km s^{-1}). On the basis of the velocity field we estimate the position angle of the major axis to lie between 15° and 55°. The H I-derived parameters are listed in Table 2.

4. OPTICAL PROPERTIES

In Fig. 9 we show a contour plot of the *B*-band image of the galaxy. The value of the outer contour is 25 *B* mag arcsec^{-2}. Position angle of the major axis and inclination were calculated by fitting ellipses to isophotes of the smoothed *I*-band image in seven intervals of 0.1 mag around D_{25}. The value of the position angle, 36.6°±3.9°, agrees with the value deduced from the H I data. The axial ratio (a/b) of the fitted ellipse is 1.25. The inclination is

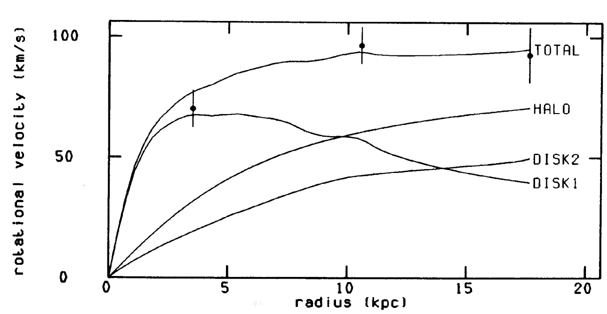

FIG. 8. Observed rotation curve of BHI 1517+39 (dots) and the rotation curves of the individual components (lines). Disks 1 and 2 are the contributions of, respectively, the stellar and the gaseous disk.

TABLE 2. Parameters of BHI 1517+39.

RA (1950)	$15^h17^m4^s$
Dec (1950)	39°49′19.8″
V_{sys}(heliocentric)	14234.2 ± 2.9 km s^{-1}
Adopted distance	145.5 Mpc
Profile width Δ_V (20%)	163.8 ± 6.8 km s^{-1}
Profile width Δ_V (50%)	126.4 ± 9.1 km s^{-1}
HI diameter D_{HI} (at 1.34×10^{20} cm^{-2})	49″ ± 2″
	34.6 ± 1.4 kpc
Largest HI extent (at $\sim 5 \times 10^{19}$ cm^{-2})	120″ ± 15″
	85 ± 11 kpc
HI mass M_{HI}	$(5.0 \pm 0.3)\ 10^9\ M_\odot$
Apparent blue magnitude m_B	17.25 ± 0.09
B-V	0.47 ± 0.10
V-I	0.76 ± 0.08
Absolute blue magnitude M_B	
(corrected for galactic absorption)	-18.59 ± 0.09
L_B	$(4.5 \pm 0.4)\ 10^9\ L_\odot$
Inclination	41.0° ± 2.8°
Position angle (major axis)	36.6° ± 3.9°
Standard diameter D_{25}	18.7″ ± 0.1″
	13.19 ± 0.07 kpc
Central surface brightness μ_0	
(corrected to face-on)	21.6 ± 0.1 B-mag arcsec^{-2}
Scale length h	1.80 ± 0.04 kpc
M_{HI}/L_B	1.1 ± 0.1
M_{dark}/M_{lum}	1.6
M_{dyn}/M_{HI}	6.9

Note to Table 2.— At 145.5 Mpc: 1″ = 0.7054 kpc.

41.0°±2.8°, including a correction for an intrinsic axial ratio of 0.2 and the 3° effect (Tully 1988).

The optical disk has an exponential light profile (Fig. 10). The profile was obtained by averaging in ellipses over the B-band image. There is no sign of a bulge, which indicates a late-type galaxy. Luminosity profiles for the V and I bands were extracted in the same way, and $B-V$ and $B-I$ color profiles were constructed. The $B-V$ profile is flat out to 10″. The $B-I$ profile shows a slight reddening of ~0.2 mag in the inner 4″, probably a result of the difference in seeing in different passbands. The extrapolated central surface brightness μ_0, after correcting for galactic extinction and line-of-sight integration, is 21.6 ± 0.1 B mag arcsec^{-2}, within the errors equal to the canonical value of 21.65 (Freeman 1970). The scale length is 2.5″, or 1.8 kpc.

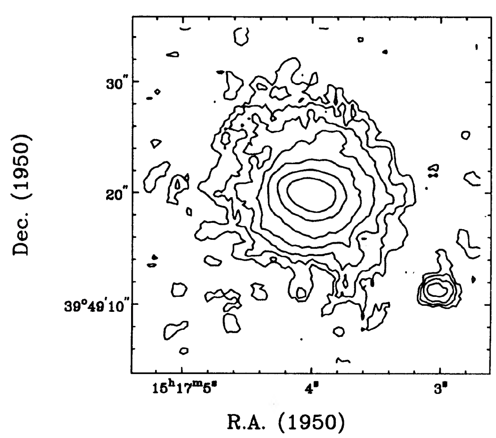

FIG. 9. Contour plot of the B-band image of BHI 1517+39, smoothed to a resolution of 1.5″. The value of the outer isophote is 25 mag arcsec^{-2}, the interval between isophotes is 0.5 mag arcsec^{-2}.

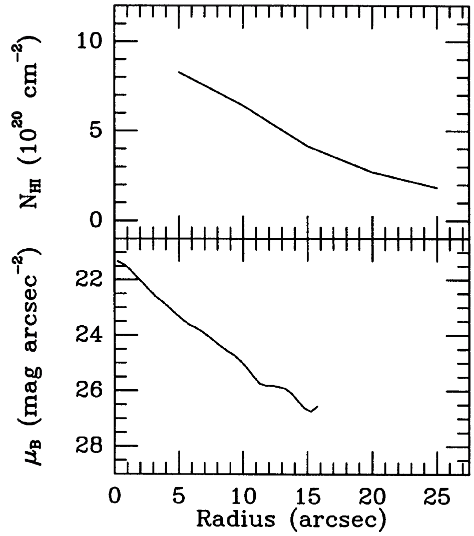

FIG. 10. Upper panel: H I column density of BHI 1517+39 as function of radius, corrected to face on. Lower panel: light profile of BHI 1517+39, obtained by an elliptical integration of the B-band image.

In the central part of the galaxy the elongation of the isophotes is more pronounced than in the outer parts (Fig. 9), while the position angle increases to about 75°. This might indicate the presence of a bar. The standard diameter D_{25} (25 B mag arcsec^{-2}, after correcting for galactic extinction and line-of-sight integration) equals 18.7″. At this isophote the smoothed B-band image shows faint extensions at both the northern and southern side of the galaxy. This, together with the barlike structure in the center, is suggestive of a very open spiral. Extrapolating the light profile to the 26.5th B mag arcsec^{-2} isophote yields a Holmberg diameter D_{Ho} of 28.3″, or 20 kpc. The optical parameters are listed in Table 2.

5. DARK MATTER CONTENT

The mass distribution of this galaxy can be determined by using the light profile, H I surface density, and the rotation curve. The rotation curve was derived from the position-velocity map (Fig. 7), the light profile and H I surface density were obtained by integrating the B-band image and total H I image in ellipses. Assuming a sech^2 law distribution in the z direction (van der Kruit & Searle 1981a, 1981b), a thickness of $0.2h$, where h is the scale length, a constant $\mathscr{M}/L$ and no internal absorption for the stellar disk and multiplying the H I column density by a factor of 1.4 to account for the presence of He, we calculated the contributions of both stellar and gas components to the rotation curve. To these components a dark isothermal halo was added and a "best" fit was made, maximizing the contribution of the stellar disk by varying its $\mathscr{M}/L$

(following the maximum disk hypothesis). The method and equations applied for making this fit have been described by Begeman (1989). Due to the large uncertainties in the observed rotation curve, the size of the core radius is not well constrained. In fact it was possible to make fits to the data varying the core radius from 1 to 20 kpc, though the fits with very small radii imply $\mathscr{M}/L$ ratios for the stellar disk of the order of 0.4. Varying the core radius from 5 to 20 kpc, the $\mathscr{M}/L$ increases from 1.4 to 1.6, with the ratio of dark to luminous mass remaining constant at 1.6.

One of the fits is shown in Fig. 8. It shows the observed rotation curve and the contribution of the individual components, stars, gas, and dark halo. The $\mathscr{M}/L$ of the stellar disk is 1.4, while the dark halo has a core radius of 5 kpc and a central density of 0.0058 $\mathscr{M}_\odot$ pc^{-3}. Within 18 kpc, the ratio of dark to luminous matter is 1.6, the ratio of dynamical to H I mass is 6.9. If the rotation curve does stay flat out to a radius of 50″, as our data suggest, this ratio is more than doubled.

It is clear, in spite of the limited quality of the data, that a dark halo, in shape and size comparable to those derived for nearby field spirals (e.g., Begeman 1987), is needed to explain the observed rotation curve.

6. DISCUSSION

6.1 Probability of Finding Companions

BHI 1517+39 was discovered as a companion to a known void galaxy, CG 1517+39. What is the chance of finding companions when observing a void galaxy? If the two-point correlation function is not drastically different in the void, the mean number of neighbors within distance R of a randomly chosen object equals

$$\langle N\rangle_p=\frac{4}{3}\pi R^3 n+n\int_0^R \xi(r)dV,$$

with n the density, $\xi(r)=(r_0/r)^\gamma$, $\gamma=1.77$, and $r_0=5.4$ Mpc (Davis & Peebles 1983).

We compute the mean galaxy density from the optical luminosity function of de Lapparent *et al.* (1988), a Schechter function with $M_B^* = -19.2$, $\alpha=-1.1$, and $\phi^*=0.02$ Mpc^{-3}. As lower cutoff we take the absolute magnitude of BHI 1517+39, -18.59. This yields a mean density of 0.0096.

BHI 1517+39 could have been detected in H I at a level of 5σ out to a radius of 17.3′ from the field center. With a total bandwidth of 3.125 MHz (effectively 530 km s^{-1}), the volume in which it could have been detected is $\sim$9 Mpc.[3]

Taking the void density to be 1/4 of the mean, the average number of neighbors in a volume of 9 Mpc^3 around a void galaxy equals 0.5. Detecting a companion of the size and luminosity of BHI 1517+39 near a known void galaxy is clearly not exceptional.

6.2 Global Properties

In this section we compare the global properties of this galaxy (listed in Table 2) to average values for field galaxies. Haynes and Giovanelli (1984) have determined average global properties for various morphological-type groupings for a sample of isolated galaxies. The average H I mass peaks at type Sb, with $\log(\mathscr{M}_{\rm H\,I})=9.67\pm0.42$, and decreases to $\log(\mathscr{M}_{\rm H\,I})=8.93\pm0.72$ for types later than Sc. The average value of $\log(\mathscr{M}_{\rm H\,I}/L_B)$ increases monotonically with Hubble type from -0.55 ± 0.41 for Sa to -0.04 ± 0.33 for >Sc. The large H I mass of BHI 1517+39 ($\log(\mathscr{M}_{\rm H\,I})=9.7$) is more typical of a Sb spiral than of an irregular. Note however that this value is only 1σ above the mean for types later than Sc. Its ratio $\log(\mathscr{M}_{\rm H\,I}/L_B)=0.04$ on the other hand strongly suggests that the galaxy is an extreme late type, in agreement with its optical appearance.

6.3 The Nature of BHI 1517+39

Does BHI 1517+39 have any properties that can be ascribed to its location in a very low density environment? This galaxy has a large H I mass and a high $\mathscr{M}_{\rm H\,I}/L_B$. It is quite blue ($B-V=0.45$), indicating active star formation. There are no color gradients; star formation seems to be distributed evenly across the disk. It is not particularly under or overluminous, which can be seen by placing it on the Tully–Fisher relation, e.g., the one derived by Richter and Huchtmeier (1984), $M_B^{0,i}=-7.17(\pm0.27)\log(\Delta V_i)-(0.82\pm0.33)$. According to this relation, a galaxy with an inclination corrected 20% velocity width of 250 km s^{-1} is expected to have an absolute magnitude of -18.

The optical appearance of BHI 1517+39 is smooth and featureless, with a slightly asymmetrical disk. There is an indication of a barlike structure in the center, and a faint suggestion of an open spiral structure. The rotation curve derived from the H I data is flat, not at all like rotation curves of irregular dwarf galaxies, which as a rule do not flatten but continue to rise. One might classify this galaxy then as a late-type spiral. Still, the absence of any obvious structure, the very low rotational velocity of the gas, and the high $\mathscr{M}_{\rm H\,I}/L_B$ make a classification of this system as irregular more likely.

Lowering the inclination to 30° would increase the rotational speed to 125 km s^{-1}, a more typical value for Sc galaxies. An error of 11° does seem rather high; of course, the optical and gas disks might have different inclinations.

None of these properties make this galaxy very remarkable. There is however one characteristic that makes it unusual. It is the size of the H I disk, which extends over at least 85 kpc. This size is enormous in absolute terms but is also unusual if compared to the optical size of the galaxy. To establish just how unique these properties are we can compare it to the properties of isolated spiral galaxies. Available data have most recently been compiled by Broeils (1992). Broeils finds that at a surface density of 1 $\mathscr{M}_\odot$ pc^{-2}, the ratio $D_{\rm H\,I}/D_{25}^{b,i}$ equals 1.8 ± 0.4. For BHI 1517+39 this ratio is 2.6, 2 σ above the mean.

At lower surface density BHI 1517+39 is more exceptional. Of course, one may wonder how much is known about H I distributions at low levels, as synthesis telescopes have only recently become sensitive enough to routinely

TABLE 3. Galaxies with extended H I disks.

Name	Type	$D_{\rm Ho}$ (kpc)	$D_{\rm H\,I}/D_{\rm Ho}$	$\Sigma_{\rm H\,I}$ (10^{19} cm^{-2})	$\mathscr{M}_{\rm H\,I}$ ($10^9\,\mathscr{M}_\odot$)	$\mathscr{M}_{\rm H\,I}/L_B$	Ref.
NGC 628	Sc(*s*)I	23.6	4.4	1.3	6.8	0.5	1
Mkn 348	S0/*a*	27.2	5.8–7.5	1.8	12	0.5	2
DDO 154	IB(*s*)*m* IV–V	2	~5	1	0.3	5.4	3
DDO 170	Im	8.6	>2	12.5	0.6	3.7	4
BHI 1517+39	Im(?)	20	4.3	~5	5	1.1	5

Notes to TABLE 3

Column 5: surface density at H I diameter. References: (1) Kamphuis & Briggs 1992, (2) Simkin *et al.* 1987, (3) Carignan & Beaulieu 1989, (4) Lake *et al.* 1990, (5) this work.

observe at those levels. Currently the best available data are those of Briggs *et al.* (1980), who did an extremely sensitive search for H I along the major axis of a number of nearby spirals. Only 3 out of 13 galaxies were found to have H I between 2 and 3 Holmberg radii, at levels of $2\text{–}3\times10^{19}$ cm^{-2}. BHI 1517+39 extends out to more than four Holmberg radii at a comparable level.

For comparison, we list parameters of a number of galaxies with extended H I disks in Table 3. Two well-known examples of isolated galaxies with very large H I disks are Mkn 348 and NGC 628 (Heckman *et al.* 1982; Simkin *et al.* 1987; Kamphuis & Briggs 1992).

Another class of objects that have large H I disks as compared to their optical size are the gas-rich dwarfs like DDO 154 (Carignan & Beaulieu 1989) and DDO 170 (Lake *et al.* 1990). These dwarfs however have much higher $\mathscr{M}_{\rm H\,I}/L_B$ ratios than BHI 1517+39. Although they have comparable $D_{\rm H\,I}/D_{\rm Ho}$ ratios, their H I masses are very much smaller. Moreover, rotation curve measurements of these dwarfs show that the luminous mass constitutes only a minor component of the total mass, quite unlike BHI 1517+39.

There is however a striking resemblance between NGC 628, MKn 348, and BHI 1517+39 in extent and mass of the H I. Also their H I surface densities at $D_{\rm Ho}$ are practically the same: e.g., 3.5 $\mathscr{M}_\odot$ pc^{-2} for NGC 628 (Wevers 1984), and 3.6 $\mathscr{M}_\odot$ pc^{-2} for BHI 1517+39 (Fig. 10). Clearly though, BHI 1517+39 is less massive than these galaxies.

In spite of being isolated, Mkn 348 and NGC 628 show some evidence of recent accretion of small companions or tidal interaction (Simkin *et al.* 1987; Kamphuis & Briggs 1992). In BHI 1517+39 the only sign of a possible disturbance is its irregular surface density distribution. This could have been caused by an interaction with its rather distant companion, CG 1517+39: a simple calculation of dynamical time scales shows that the relative velocity of these galaxies should be of the order of 500 km s^{-1} for an interaction to have taken place some three orbital periods ago.

Most galaxies that are known to have extended H I are either clearly interacting or in the process of merging. BHI 1517+39, however, does not have any of the characteristics of a major interaction, such as tidal bridges or tails, enhanced infrared and radio emission.

We thus conclude that BHI 1517+39 belongs to the class of rare objects that have large, relatively undisturbed, low surface density H I disks. These galaxies all seem to be rather isolated; it would be expected that such objects, with their extended, dynamically fragile disks, could survive to the present epoch in low density regions, free from encounters with other massive galaxies.

Why don't these disks form stars? Kennicutt (1989) has shown that the star formation threshold appears to be associated with the onset of large-scale gravitational instabilities in the gaseous disk. In Fig. 10 we plot the average H I surface density, corrected to face on, as a function of radius. Following Kennicutt (1989) the stability condition in a differentially rotating disk with a flat rotation curve has the following form:

$$\Sigma_{\rm crit}(\mathscr{M}_\odot{\rm pc}^{-2})=0.44\alpha V({\rm km\ s}^{-1})/R({\rm kpc}),$$

where R is the radius and V the rotational speed of the disk at that radius. The value of α may be determined by normalizing the ratio $\Sigma_{\rm gas}/\Sigma_{\rm crit}$ at the edge of the star-forming disk. For late-type galaxies, α ranges between 0.5 and 0.85, with an average of 0.67.

We have calculated $\Sigma_{\rm gas}/\Sigma_{\rm crit}$ for the outer two points, where the rotation curve could still be measured, using the H I column density multiplied by 1.4 to include other elements. The values of this ratio at 15″ and 25″ are, respectively, $1.2/\alpha$ and $0.9/\alpha$. Clearly most of the low surface brightness disk farther out has gas densities well below the critical value (assuming the rotation curve stays flat), so that massive star formation will be suppressed.

The existence of such a large extent of H I raises the possibility of a low surface brightness stellar disk. There are some nonstellar objects to the south of BHI 1517+39 which could be either dwarf satellites or possibly H II regions embedded in a low surface brightness disk. If the latter, this object might in the outer parts be a smaller version of the giant low surface brightness galaxy Malin I (Bothun *et al.* 1987); much deeper images are needed to confirm such a speculation.

Hoffman *et al.* (1992) investigate the influence of the large-scale environment on the structure of galaxies. They claim that the structure of dwarf galaxies, associated with 1σ fluctuations, will be relatively unaffected by their environment. The structure of rare ($\sim3\sigma$) massive galaxies though should be strongly dependent on the surrounding density, with massive low surface-brightness galaxies, like

Malin I and II, forming in voids. The cooling time in the outer parts of such galaxies will be larger than the dynamical time, causing the disks to be relatively unevolved, while the central parts develop normally and undergo rapid star formation.

BHI 1517+39 is clearly not a low surface-brightness galaxy and does not lie in the same mass range as Malin I and II. Malin I has a H I mass nine times larger than BHI 1517+39, a rotational velocity of 140 km s^{-1}, and a H I extent of about 160 kpc (van Gorkom *et al.* 1992). It does resemble BHI 1517+39 in its $\mathscr{M}_{\rm H\,I}/L_B$ ratio of 1. In view of this it is rather remarkable that the large, unevolved gaseous disk, and seemingly normal central region of BHI 1517+39 agree so well with the properties predicted for massive void galaxies.

7. SUMMARY, CONCLUSIONS

We have observed a H I-discovered galaxy located in the Bootes void at low and high resolution in the 21 cm line and optically find it to be an irregular, with a high $\mathscr{M}_{\rm H\,I}/L_B$ of 1.1 and a $D_{\rm H\,I}/D_{25}$ of 6.4. The galaxy has a slowly rotating H I disk, which extends in places to a radius of 45 kpc. The H I distribution at high resolution appears irregular. This may have been caused by a tidal interaction with a remote companion, CG 1517+39. Considering the shape of the velocity field and the low resolution H I data, we think it more probable that the extended emission is part of a warped, low surface density disk, rotating at constant speed. The existence of such an extended disk may be a consequence of the relative isolation of this object in the void. A low surface-brightness stellar disk may exist as well, similar to Malin I, but much deeper images are needed to assess this possibility.

The rotation curve of this galaxy is flat and can be explained by adding a "standard" dark halo, similar to those derived for nearby spirals.

We thank the NRAO for generous allocation of observing time. We also thank Renzo Sancisi and Tjeerd van Albada for stimulating discussions and suggestions, and René Oudmaijer for a critical reading of the manuscript. This research was partly supported by NSF grants to Columbia University, by the Netherlands Foundation for Research in Astronomy (NFRA), and the Netherlands Organization for Scientific Research (NWO) under Grant Nos. 782-373-046 and 782-373-044. The JKT is operated on the island of La Palma by the Royal Greenwich Observatory in the Spanish Observatorio del Roque de los Muchachos of the Instituto de Astrofisica de Canarias.

REFERENCES

Begeman, K. 1987, Ph.D. thesis, University of Groningen, The Netherlands
Begeman, K. 1989, A&A, 223, 47–60
Bosma, A. 1981, AJ, 86, 1791
Bothun, G. D., & Aldering, G. 1988, BAAS, 20, 1087
Bothun, G. D., Impey, C. D., Malin, D. F., & Mould, J. R. 1987, AJ, 94(1), 23
Broeils, A. H. 1992, Ph.D. thesis, University of Groningen, The Netherlands
Burstein, D., & Heiles, C. 1984, ApJS, 54, 33
Carignan, C., & Beaulieu, S. 1989, ApJ, 347, 760–770
Cristian, C. A., Adams, M., Barnes, J. V., Butcher, H., Hayes, D. S., Mould, J. R., & Siegel, M. 1985, PASP, 97, 363
Davis, M., & Peebles, P. J. E. 1983, ApJ, 267, 465–482
de Lapparent, V., Geller, M. J., & Huchra, J. P. 1988, ApJ, 343, 1
Dey, A., Strauss, M. A., & Huchra, J. P. 1990, AJ, 99, 463
Dressler, A. 1980, ApJ, 236, 351
Freeman, K. C. 1970, ApJ, 160, 811
Haynes, M. P., & Giovanelli, R. 1984, AJ, 89, 758
Heckman, T. M., Sancisi, R., Sullivan, W. T., & Balick, B. 1982, MNRAS, 199, 425–433
Hoffman, Y., Silk, J., & Wyse, R. F. G. 1992, ApJ, 388, L13–L17
Kamphuis, J., & Briggs, F. 1992, A&A, 253, 335–348
Kennicutt, R. C. 1989, ApJ, 344, 685
Kirshner, R. P., Oemler, A., Schechter, P. L., & Shectman, S. A. 1981, ApJ, 248, L57
Kirshner, R. P., Oemler, A., Schechter, P. L., & Shectman, S. A. 1987, ApJ, 314, 493
Lake, G., Schommer, R. A., & van Gorkom, J. H. 1990, AJ, 99, 547
Moody, J. W. 1986, Ph.D. thesis, University of Michigan
Moody, J. W., Kirshner, R. P., MacAlpine, G. M., & Gregory, S. A. 1987, ApJ, 314, L33
Napier, P. J., Thompson, A. R., Ekers, R. D. 1983, Proceedings Inst. Electron. Electr. Eng. 71, 1295
Oemler, A. 1974, ApJ, 194, 1
Postman, M., & Geller, M. J. 1983, ApJ, 281, 95
Richter, O. G., & Huchtmeier, W. K. 1984, A&A, 132, 253
Sandage, A. 1975, in Galaxies and the Universe, edited by A. Sandage, M. Sandage, and J. Kristian (University of Chicage Press, Chicago)
Sanduleak, N., & Pesch, P. 1982, ApJ, 258, L11
Sanduleak, N., & Pesch, P. 1987, ApJS, 63, 809
Schild, R. E. 1983, PASP, 95, 1021
Simkin, S. M., van Gorkom, J. H., Hibbard, J., & Su, H.-J. 1987, Science, 235, 1367
Szomoru, A., Gregg, M., & van Gorkom, J. H. 1993, in preparation
Tifft, W. G., Kirshner, R. P., Gregory, S. P., & Moody, J. W. 1986, ApJ, 310, 505
Tully, B. 1988, Nearby Galaxies Catalog (Cambridge University Press, Cambridge)
Tyson, N. D., & Scalo, J. M. 1988, ApJ, 329, 618
van der Kruit, P. C., & Searle, L. 1981a, A&A, 95, 105
van der Kruit, P. C., & Searle, L. 1981b, A&A, 95, 116
van Gorkom, J. H., Bothun, G. D., & Impey, C. D. 1992, in preparation
Weistrop, D. 1987, BAAS, 19, 1074
Weistrop, D., & Downes, R. A. 1988, ApJ, 331, 172
Wevers, B.M.H.R. 1984, Ph.D. thesis, University of Groningen, The Netherlands